

This work was written as part of one of the author's official duties as an Employee of the United States Government and is therefore a work of the United States Government. In accordance with 17 U.S.C. 105, no copyright protection is available for such works under U.S. Law.

Public Domain Mark 1.0

<https://creativecommons.org/publicdomain/mark/1.0/>

Access to this work was provided by the University of Maryland, Baltimore County (UMBC) ScholarWorks@UMBC digital repository on the Maryland Shared Open Access (MD-SOAR) platform.

Please provide feedback

Please support the ScholarWorks@UMBC repository by emailing scholarworks-group@umbc.edu and telling us what having access to this work means to you and why it's important to you. Thank you.

PAPER

CALET on the International Space Station: the first three years of observations






To cite this article: P Brogi *et al* 2020 *Phys. Scr.* **95** 074012

View the [article online](#) for updates and enhancements.

You may also like

- [Monte Carlo Study of Electron and Positron Cosmic-Ray Propagation with the CALET Spectrum](#)
Katsuaki Asano, Yoichi Asaoka, Yosui Akaike et al.
- [Search for GeV Gamma-Ray Counterparts of Gravitational Wave Events by CALET](#)
O. Adriani, Y. Akaike, K. Asano et al.
- [CALET's sensitivity to Dark Matter annihilation in the galactic halo](#)
H. Motz, Y. Asaoka, S. Torii et al.

CALET on the International Space Station: the first three years of observations

P Brogi^{1,2} , O Adriani^{3,4}, Y Akaike^{5,6}, K Asano⁷ , Y Asaoka^{8,9}, M G Bagliesi^{1,2}, E Berti^{3,4}, G Bigongiari^{1,2}, W R Binns¹⁰, S Bonechi^{1,2}, M Bongi^{3,4}, A Bruno¹¹, J H Buckley¹⁰, N Cannady^{5,6} , G Castellini¹², C Checchia^{3,4}, M L Cherry¹³, G Collazuol^{14,15}, V Di Felice^{16,17}, K Ebisawa¹⁸, H Fuke¹⁸ , T G Guzik¹³, T Hams^{5,6}, K Hibino¹⁹, M Ichimura²⁰, K Ioka²¹, W Ishizaki⁷, M H Israel¹⁰, K Kasahara⁸, J Kataoka⁸, R Kataoka²², Y Katayose²³, C Kato²⁴, N Kawanaka^{25,26}, Y Kawakubo¹³, K Kohri²⁷, H S Krawczynski¹⁰, J F Krizmanic^{5,6}, J Link^{5,6}, P Maestro^{1,2}, P S Marrocchesi^{1,2}, A M Messineo^{2,28}, J W Mitchell²⁹, S Miyake³⁰, A A Moiseev^{5,31}, M Mori³², N Mori⁴ , H M Motz³³, K Munakata²⁴, H Murakami⁸, S Nakahira³⁴, J Nishimura¹⁸, G A de Nolfo¹¹, S Okuno¹⁹, J F Ormes³⁵, N Ospina^{14,15} , S Ozawa⁸, L Pacini⁴, F Palma^{16,17}, P Papini⁴, B F Rauch¹⁰, S B Ricciarini^{4,12}, K Sakai^{5,6}, T Sakamoto³⁶, M Sasaki^{5,31}, Y Shimizu¹⁹, A Shiomii³⁷, R Sparvoli^{16,17}, P Spillantini³, F Stolzi^{1,2}, S Sugita³⁶, J E Suh^{1,2}, A Sulaj^{1,2}, I Takahashi³⁸, M Takita⁷, T Tamura¹⁹, T Terasawa³⁴, S Torii^{8,39}, Y Tsunesada⁴⁰ , Y Uchihori⁴¹, E Vannuccini⁴, J P Wefel¹³, K Yamaoka⁴², S Yanagita⁴³, A Yoshida³⁶ and K Yoshida⁴⁴

¹ Department of Physical Sciences, Earth and Environment, University of Siena, via Roma 56, 53100 Siena, Italy

² INFN Sezione di Pisa, Polo Fibonacci, Largo B. Pontecorvo, 3-56127 Pisa, Italy

³ Department of Physics, University of Florence, Via Sansone, 1-50019 Sesto Fiorentino, Italy

⁴ INFN Sezione di Florence, Via Sansone, 1-50019 Sesto Fiorentino, Italy

⁵ CRESST and Astroparticle Physics Laboratory NASA/GSFC, Greenbelt, MD 20771, United States of America

⁶ Department of Physics, University of Maryland, Baltimore County, 1000 Hilltop Circle, Baltimore, MD 21250, United States of America

⁷ Institute for Cosmic Ray Research, The University of Tokyo, 5-1-5 Kashiwa-no-Ha, Kashiwa, Chiba 277-8582, Japan

⁸ Research Institute for Science and Engineering, Waseda University, 3-4-1 Okubo, Shinjuku, Tokyo 169-8555, Japan

⁹ JEM Utilization Center, Human Spaceflight Technology Directorate, Japan Aerospace Exploration Agency, 2-1-1 Sengen, Tsukuba, Ibaraki 305-8505, Japan

¹⁰ Department of Physics, Washington University, One Brookings Drive, St. Louis, MO 63130-4899, United States of America

¹¹ Heliospheric Science Division, NASA/Goddard Space Flight Center—Code 672, Bldg. 21, Room 137D, Greenbelt MD 20771, United States of America

¹² Institute of Applied Physics (IFAC), National Research Council (CNR), Via Madonna del Piano, 10, 50019 Sesto Fiorentino, Italy

¹³ Department of Physics and Astronomy, Louisiana State University, 202 Nicholson Hall, Baton Rouge, LA 70803, United States of America

¹⁴ Department of Physics and Astronomy, University of Padova, Via Marzolo, 8, 35131 Padova, Italy

¹⁵ INFN Sezione di Padova, Via Marzolo, 8, 35131 Padova, Italy

¹⁶ University of Rome ‘Tor Vergata’, Via della Ricerca Scientifica 1, 00133 Rome, Italy

¹⁷ INFN Sezione di Rome ‘Tor Vergata’, Via della Ricerca Scientifica 1, 00133 Rome, Italy

¹⁸ Institute of Space and Astronautical Science, Japan Aerospace Exploration Agency, 3-1-1 Yoshinodai, Chuo, Sagami-hara, Kanagawa 252-5210, Japan

¹⁹ Kanagawa University, 3-27-1 Rokkakubashi, Kanagawa, Yokohama, Kanagawa 221-8686, Japan

²⁰ Faculty of Science and Technology, Graduate School of Science and Technology, Hirosaki University, 3, Bunkyo, Hirosaki, Aomori 036-8561, Japan

- ²¹ Yukawa Institute for Theoretical Physics, Kyoto University, Kitashirakawa Oiwakecho, Sakyo, Kyoto 606-8502, Japan
- ²² National Institute of Polar Research, 10-3, Midori-cho, Tachikawa, Tokyo 190-8518, Japan
- ²³ Faculty of Engineering, Division of Intelligent Systems Engineering, Yokohama National University, 79-5 Tokiwadai, Hodogaya, Yokohama 240-8501, Japan
- ²⁴ Faculty of Science, Shinshu University, 3-1-1 Asahi, Matsumoto, Nagano 390-8621, Japan
- ²⁵ Hakubi Center, Kyoto University, Yoshida Honmachi, Sakyo-ku, Kyoto 606-8501, Japan
- ²⁶ Department of Astronomy, Graduate School of Science, Kyoto University, Kitashirakawa Oiwakecho, Sakyo-ku, Kyoto 606-8502, Japan
- ²⁷ Institute of Particle and Nuclear Studies, High Energy Accelerator Research Organization, 1-1 Oho, Tsukuba, Ibaraki 305-0801, Japan
- ²⁸ University of Pisa, Polo Fibonacci, Largo B. Pontecorvo, 3-56127 Pisa, Italy
- ²⁹ Astroparticle Physics Laboratory, NASA/GSFC, Greenbelt, MD 20771, United States of America
- ³⁰ Department of Electrical and Electronic Systems Engineering, National Institute of Technology, Ibaraki College, 866 Nakane, Hitachinaka, Ibaraki 312-8508 Japan
- ³¹ Department of Astronomy, University of Maryland, College Park, Maryland 20742, United States of America
- ³² Department of Physical Sciences, College of Science and Engineering, Ritsumeikan University, Shiga 525-8577, Japan
- ³³ International Center for Science and Engineering Programs, Waseda University, 3-4-1 Okubo, Shinjuku, Tokyo 169-8555, Japan
- ³⁴ RIKEN, 2-1 Hirosawa, Wako, Saitama 351-0198, Japan
- ³⁵ Department of Physics and Astronomy, University of Denver, Physics Building, Room 211, 2112 East Wesley Avenue, Denver, Colorado 80208-6900, United States of America
- ³⁶ College of Science and Engineering, Department of Physics and Mathematics, Aoyama Gakuin University, 5-10-1 Fuchinobe, Chuo, Sagami-hara, Kanagawa 252-5258, Japan
- ³⁷ College of Industrial Technology, Nihon University, 1-2-1 Izumi, Narashino, Chiba 275-8575, Japan
- ³⁸ Kavli Institute for the Physics and Mathematics of the Universe, The University of Tokyo, 5-1-5 Kashiwanoha, Kashiwa, 277-8583, Japan
- ³⁹ School of Advanced Science and Engineering, Waseda University, 3-4-1 Okubo, Shinjuku, Tokyo 169-8555, Japan
- ⁴⁰ Division of Mathematics and Physics, Graduate School of Science, Osaka City University, 3-3-138 Sugimoto, Sumiyoshi, Osaka 558-8585, Japan
- ⁴¹ National Institutes for Quantum and Radiation Science and Technology, 4-9-1 Anagawa, Inage, Chiba 263-8555, Japan
- ⁴² Nagoya University, Furo, Chikusa, Nagoya 464-8601, Japan
- ⁴³ College of Science, Ibaraki University, 2-1-1 Bunkyo, Mito, Ibaraki 310-8512, Japan
- ⁴⁴ Department of Electronic Information Systems, Shibaura Institute of Technology, 307 Fukasaku, Minuma, Saitama 337-8570, Japan

E-mail: paolo.brogi@unisi.it

Received 27 February 2020, revised 28 April 2020

Accepted for publication 21 May 2020

Published 29 May 2020



Abstract

The CALorimetric Electron Telescope CALET is a space instrument designed to carry out precision measurements of high energy cosmic-rays on the JEM-EF external platform on the International Space Station, where it has been collecting science data continuously since mid October 2015. In addition to its primary goal of identifying nearby sources of high-energy electrons and possible signatures of dark matter in the electron spectrum, CALET is carrying out extensive measurements of the energy spectra, relative abundances and secondary-to-primary ratios of elements from proton to iron, and even above (up to $Z = 40$), studying the details of galactic particle propagation and acceleration. An overview of CALET based on the data taken during the first three years of observations is presented, including a direct measurement of the electron+positron energy spectrum from 11 GeV to 4.8 TeV. The proton spectrum has been measured from 50 GeV to 10 TeV covering, for the first time with a single space-borne instrument, the whole energy interval previously investigated in separate sub-ranges by magnetic spectrometers and calorimetric instruments. Preliminary spectra of cosmic-ray nuclei are also

presented, together with gamma-ray observations and searches for an e.m. counterpart of LIGO/Virgo GW events.

Keywords: Cosmic rays, CALET, electron, nuclei, gamma rays

(Some figures may appear in colour only in the online journal)

1. Introduction

The CALorimetric Electron Telescope (CALET) [1–3] is a space experiment developed and operated by an international collaboration led by the Japanese Space Agency (JAXA) with the participation of the Italian Space Agency (ASI) and NASA.

The CALET detector was launched on 19 August 2015, with the Japanese carrier H-II, delivered to the International Space Station by the HTV-5 Transfer Vehicle, and installed on the Japanese Experiment Module Exposure Facility (JEM-EF).

The main goal of CALET science program is to search signatures of nearby cosmic-ray (CR) sources and possibly dark matter, by measuring accurately the spectrum of electron (including positron) and gamma-rays up to 20 TeV. Moreover, CALET will also investigate: the origin of cosmic-rays; the study of their acceleration mechanism(s) and the propagation of primary and secondary elements in the Galaxy. In fact the design of the CALET instrument has been optimized to allow precision measurements of the energy spectra and the relative abundances of light and heavy cosmic nuclei (from proton to iron) in CRs, up to the highest energies ever directly observed (approaching the PeV region). A specific study is dedicated to the measurements of trans-iron elements abundances (up to $Z = 40$) with a long term observations program.

The CALET telescope has an instrument (CGBM) dedicated to gamma-ray transients detection, that covers the energy range 7 keV – 20 MeV, and could be used, in combination with the calorimeter, to perform the search of counterpart emission related to gravitational wave events [4–6].

In this paper, we report the extended measurement of the inclusive electron+positron spectrum from 10 GeV up to 4.8 TeV [7] and the recent direct measurement of the proton spectrum in the energy range from 50 GeV to 10 TeV [8], after 3 years of operations on the ISS. We also summarize the present status of other CALET measurements.

2. The CALET telescope

The CALET main telescope, that is shown in figure 1 together with the entire CALET payload, is an all-calorimetric instrument, that consists of three sub-detectors.

The CHarge Detector (CHD), that is positioned at the top of the apparatus and consists of a two layer hodoscope of plastic scintillators paddles (14 paddles for each layer). This first sub-detector performs the charge identification of individual nuclear species, providing a measurement of the charge Z of the incident particle over a wide dynamic range (from

$Z = 1$ up to $Z = 40$) with sufficient charge resolution to resolve individual elements [9].

The IMaging Calorimeter (IMC), a fine grained sampling calorimeter segmented longitudinally into 16 layers of scintillating fibers (with 1 mm^2 square cross-section) read-out individually and arranged in pairs along orthogonal directions, each pair is interleaved with thin tungsten absorbers (for a total thickness of $3 X_0$). It is used to reconstruct the early shower profile and the impinging particle trajectory with good angular resolution (about 0.1° for electrons and less than 0.5° for hadrons) [10]. Moreover, the IMC performs a redundant charge measurement via multiple dE/dx measurements along the primary track [11].

The third detector is the Total AbSorption Calorimeter (TASC), an homogeneous calorimeter made of 12 layers of lead-tungstate (PWO) logs, arranged in pairs along $x - y$ directions, and capable, with its $27 X_0$ thickness and its shower imaging capability, to measure electrons and gamma-rays with an excellent energy resolution, providing high discrimination against hadronic cascades.

The total thickness of the main telescope is equivalent to $30 X_0$ and 1.3 proton interaction lengths (λ_I), the geometrical factor is $0.12 \text{ m}^2 \text{ sr}$. A more detailed description of the instrument can be found in [12] and in the Supplemental Material (SM) of [13].

3. In orbit operations and calibrations

3.1. In orbit operations

After the successful launch on 19 August 2015 and the installation on the JEM-EF on 25 August, the CALET instrument started its commissioning phase aboard the ISS, that was successfully completed at beginning of October 2015. Since then the CALET detector has been taking science data with smooth and continuous operations, without any major interruption [14].

The Waseda CALET Operations Center (WCOC) located at Waseda University (Tokyo) controls the CALET in orbit operations, via the JAXA Ground Support Equipment (JAXA-GSE) located at the Tsukuba Space Center. The total observation time was 1327 days as of 31 May 2019, with a live time fraction of about 84% and more than 860 million events observed in High-Energy (HE) trigger mode. HE trigger is a continuously active trigger mode conceived to ensure maximum exposure to electrons (above 10 GeV) and other high-energy shower events. The CALET cumulative observation time is shown in figure 2 (black line), together with the cumulative live time (red) and dead time (blue). As shown, the cumulative observation/live time has a smooth

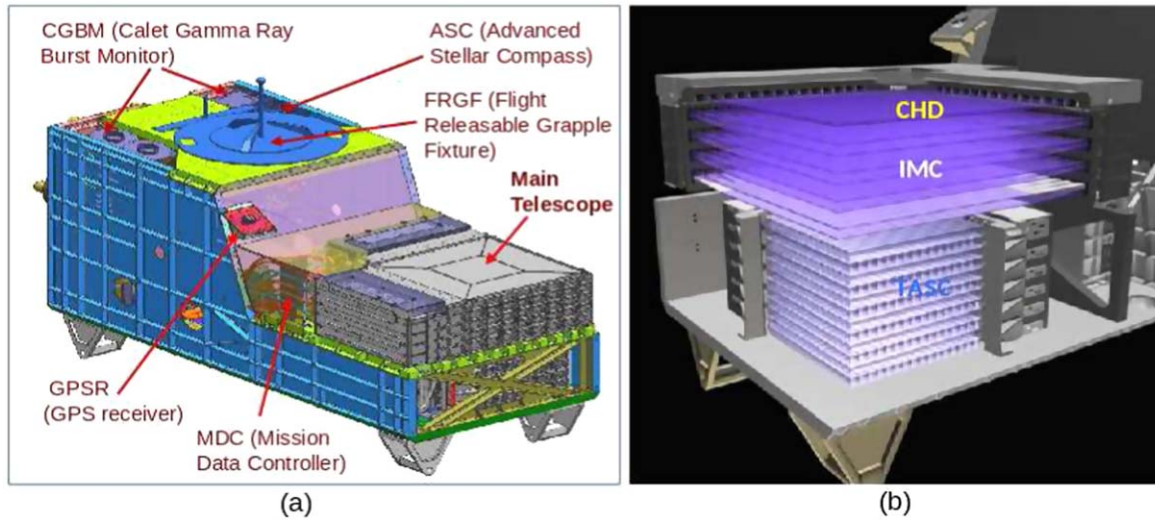


Figure 1. (a) CALET payload; (b) telescope layout with details of the three sub-detectors.

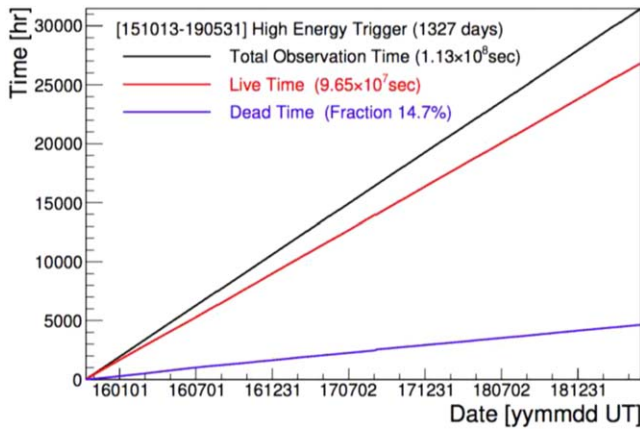


Figure 2. Cumulative observation time (black line), live time (red line) and dead time (blue line) of HE trigger mode for 1327 days of observation with CALET. Reproduced with permission from [15].

increase with no significant interruptions since the start of scientific operation [15].

3.2. In orbit calibrations

A detailed, in-flight, energy calibration is performed for each channel of CHD, IMC, and TASC, using penetrating proton and He particles, selected by a dedicated trigger mode. The light output non-uniformity is corrected as well as the gain differences among the channels, position/temperature dependence and temporal gain variations occurring in long-term observations. Moreover, the linearity over each of the four gain ranges is confirmed for each TASC channel, the responses from neighboring ranges are linked to ensure a seamless transition.

This results in a very high resolution of about 2% or even better above 20 GeV [12], with a dynamic range of more than six orders of magnitude, that allows to observe from minimum ionizing protons to 1 PeV showers. Nevertheless, even though this calibration is extensive, its uncertainty is a

limiting factor for the energy resolution (the intrinsic resolution is expected to be $\sim 1\%$) and the calibration error in the lower gain ranges is critical for spectrum measurements in the TeV range.

4. CALET results after the first three years

4.1. Total electron spectrum

One of the CALET main science goals is the precise measurement of the all-electron (electron+positron) spectrum up to the TeV region, in order to possibly detect fine structures that could reveal the presence of a nearby cosmic-ray source, providing its first experimental evidence [16, 17].

Moreover, the explanation of the unexpected increase of the positron fraction as suggested by magnetic spectrometer balloon data [18], and references therein and confirmed by the precise measurements of PAMELA [19] and AMS-02 [20], might indicate the presence of a primary source for positrons (in addition to their generally accepted secondary origin). Primary source candidates span from astrophysical (pulsar) to exotic components like dark matter (DM), and since these primary sources emit electron-positron pairs, it is expected that the total electron spectrum will exhibit a spectral feature near the highest energy range of the primary component.

The electron identification is performed by taking advantage of the 30 X_0 thick calorimeter that allows full containment of electron shower events at TeV scale (with excellent energy resolution, $< 2\%$ at energy above 20 GeV), exploiting the shape difference between electromagnetic and hadronic shower.

For electron analysis [7, 13] (and supplement material of [7, 13]), the data sample is pre-selected to obtain well-reconstructed and well-contained single-charged events, applying: offline trigger confirmation; geometrical condition; a track quality cut to ensure reconstruction accuracy; charge selection using CHD and requiring the longitudinal shower

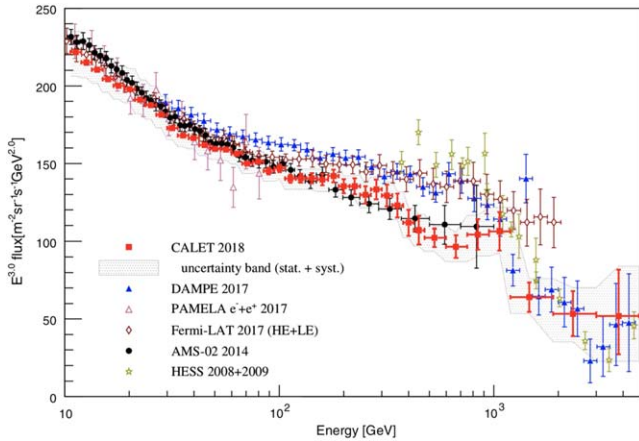


Figure 3. Cosmic-ray all-electron spectrum measured by CALET from 11 GeV to 4.8 TeV [7]. The error bars along the horizontal and vertical axes indicate bin width and statistical errors, respectively. The gray band indicates the quadratic sum of statistical and systematic errors (not including the uncertainty on the energy scale). Other direct measurements in space are plotted for comparison [21–24], as well as from ground-based experiments [25, 26]. Reprinted (figure) with permission from [7], Copyright (2018) by the American Physical Society.

development and lateral shower containment to be consistent with those expected for electromagnetic cascades. Then the electron selection is performed applying two methods: a simple two parameter cuts and multivariate analysis (MVA) based on machine learning (the boosted decision tree method from TMVA toolkit is used). The overall selection efficiency results greater than 70% above 30 GeV, when the efficiency of electron selection cut is fixed at 80%, while the trigger is almost fully efficient above ~ 100 GeV, and the cuts on geometrical condition, track quality, charge selection and shower development consistency have an overall efficiency greater than 90% above 30 GeV (see supplement material of [13]).

The CALET collaboration has published its first results on electrons in the energy range of 10 GeV to 3 TeV [13] on November 2017, then an updated version (based on 780 days of flight data and the full geometrical acceptance) followed recently, extending the energy range up to 4.8 TeV [7]. Figure 3 shows the updated electron spectrum measured by CALET, in this second analysis [7], using the same energy binning as that used in our previous publication [13], except one additional energy bin between 3 and 4.8 TeV. The spectra from the two papers are perfectly consistent bin-by-bin within the errors, but with respect to the previous analysis the updated version has a doubled statistics at $E > 475$ GeV. The resultant contamination ratios of protons in the final electron sample are $\sim 1\%$ up to 1 TeV, and 10%–20% in the 1–4.8 TeV region, while keeping a constant high efficiency of 80% for electrons [7].

The CALET electron spectrum results to be consistent with AMS-02 data [24] below 1 TeV, despite the two detectors use different detection techniques to identify electron up to the TeV (calorimeter versus magnetic spectrometer). On the other hand, the CALET and AMS-02 measurements results significantly softer than the spectra reported by Fermi/LAT [23] and DAMPE [21], in the energy region from 300 to

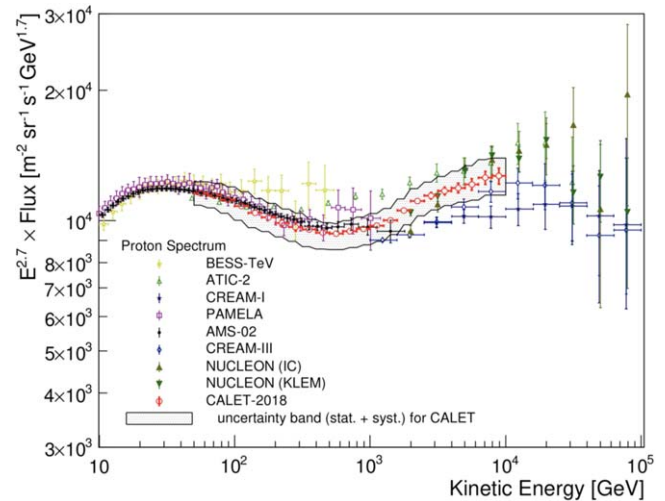


Figure 4. First CALET measurement of the CR proton spectrum from 50 GeV to 10 TeV [8]. The gray band indicates the quadratic sum of statistical and systematic errors. Also plotted are recent direct measurements [27, 32–36]. Reproduced from [8]. CC BY 4.0.

600 GeV. This might suggest the presence of unknown systematic errors. Nevertheless, above 1 TeV, CALET observes a flux suppression that is consistent with DAMPE within errors.

Several theoretical speculations have been made about the origin of a peak-like structure near 1.4 TeV in the DAMPE data, instead, CALET does not observe any significant evidence for a narrow spectral feature in this energy region. The results of the two experiments, in the cosmic-ray all-electron spectrum around 1.4 TeV, differ at level of 4σ significance (including the systematic errors from both experiments).

4.2. Proton spectrum

Protons are the most abundant charged particles in cosmic-rays. The measurements of the precise behavior of the proton spectrum are important to provide information, complementary to electron observations, to understand the origin, acceleration, and propagation of cosmic-rays. In particular, following the recent observations of a spectral hardening in proton [27] and in heavier nuclei spectra [28–31], it becomes of particular interest to investigate the region of spectral break-point and measure accurately the energy dependence of the spectral index.

The CALET experiment, thanks to its wide dynamic range, allows for the study of the detailed shape of the spectrum, covering, for the first time with a single experimental apparatus in space, the whole energy range previously investigated by magnetic spectrometers [27, 29, 32] and calorimetric instruments [33–36], which normally cover separate sub-ranges of the region explored so far by CALET.

Figure 4 shows the first measurement of the proton spectrum by CALET [8], in the wide energy range from 50 GeV to 10 TeV. The analyzed flight data were collected from 13 October 2015 to 31 August 2018 for a total observation time of 21 421.9 hours for HE trigger mode (with a live time fraction of 84.7%), and an additional live time of

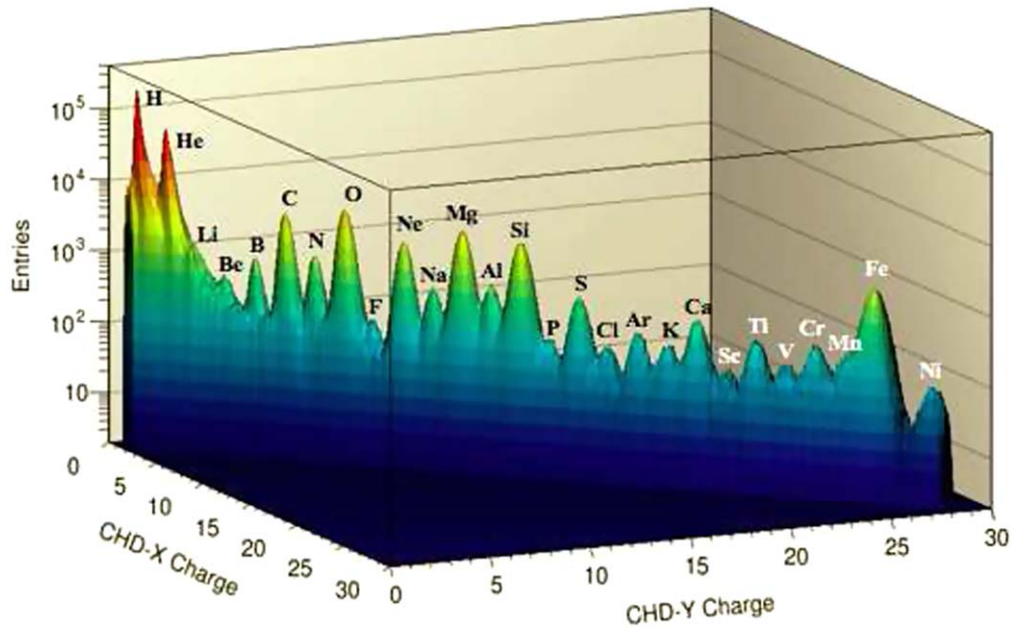


Figure 5. CHD charge separation capability, using CHD-X and CHD-Y charge measurements. Reproduced from [37]. © IOP Publishing Ltd. CC BY 3.0.

365.4 hours for low-energy (LE) shower trigger [14] used to extend the energy coverage in the lower-energy region from 50 GeV to ~ 300 GeV.

A pre-selection is applied to identify well-reconstructed and well-contained events and remove events not included in the Monte Carlo (MC) samples (i.e. events with incidence from the zenith angle greater than 90° and mis-reconstructed events). The pre-selection consisted of: offline trigger confirmation; geometrical condition; track quality cut; electron rejection cut; off-acceptance event rejection cut; requirement of track consistency with TASC energy deposits and shower development requirement in IMC. The thresholds of the last two cuts are energy dependent and are chosen to maintain a constant selection efficiency of 95% and 99% respectively, on the whole energy range. The efficiency of the electron rejection cut for protons is above 92%. Track quality and off-acceptance rejection cuts are highly efficient. The overall efficiency of proton selection is shown in details in figure 3 of [8] as effective acceptance depending on the trigger selection. Then, the charge selection is performed on the preselected samples to identify particles with $Z = 1$. Charge identification consists of simultaneous window cuts on CHD and IMC reconstructed charges, chosen to achieve a 95% selection efficiency for all energies. Subsequently, the small residual contamination (not exceeding 5%), from background related to off-acceptance protons or misidentified helium or electron events, is subtracted and energy unfolding is performed to correct for bin migration related to the limited energy resolution (30%–40% for hadronic showers). Finally, taking into account the event selection efficiency, geometrical factor and live time, the cosmic-ray proton spectrum is derived. The systematic uncertainties were studied in detail, as well, and the total uncertainty results to be less than 10% over the whole energy range. For a detailed description of this analysis see [8] Supplemental Material of [8].

The CALET proton spectrum (figure 4) results consistent with the very accurate magnetic spectrometer measurement by AMS-02 [27] below 1 TeV and with measurements from calorimetric instruments (like CREAM-III [35]) in the high-energy region. Our measurement confirms the presence of spectral hardening above a few hundreds GeV, providing evidence of a deviation from a single power-law by more than 3σ , and showing a very smooth transition of the power-law spectral index from -2.81 ± 0.03 in the energy region 50–500 GeV to -2.56 ± 0.04 between 1 and 10 TeV.

4.3. Heavy and Ultra Heavy nuclei observation

CALET, thanks to its wide dynamic range, $30 X_0$ thickness and excellent charge identification capability, it is capable of carry out extensive measurements of the energy spectra and secondary-to-primary ratios of cosmic-ray heavy nuclei up to iron. Figure 5 shows the charge identification capability of CALET (using the CHD detector only), that can clearly separate each nuclear species up to iron and nickel. Preliminary results of carbon, oxygen, neon, magnesium, silicon, iron spectra and B/C flux ratio were recently presented in [37, 38] and [39].

In addition to heavy nuclei spectra measurements, CALET has the capability to measure Ultra-Heavy Cosmic-Ray (UHCN) nuclei ($Z > 26$), up to zirconium ($Z = 40$). Thanks to a dedicated UHCN trigger, that provides an expanded geometric acceptance, about 6 times larger than for events fully contained by the calorimeter, the CALET experiment will collect (in ~ 5 years) a data set comparable to that collected so far by the balloon-borne SuperTIGER instrument [40]. Preliminary CALET results presented in [41] are in reasonable agreement with SuperTIGER relative abundances of UHCN nuclei in a similar energy range.

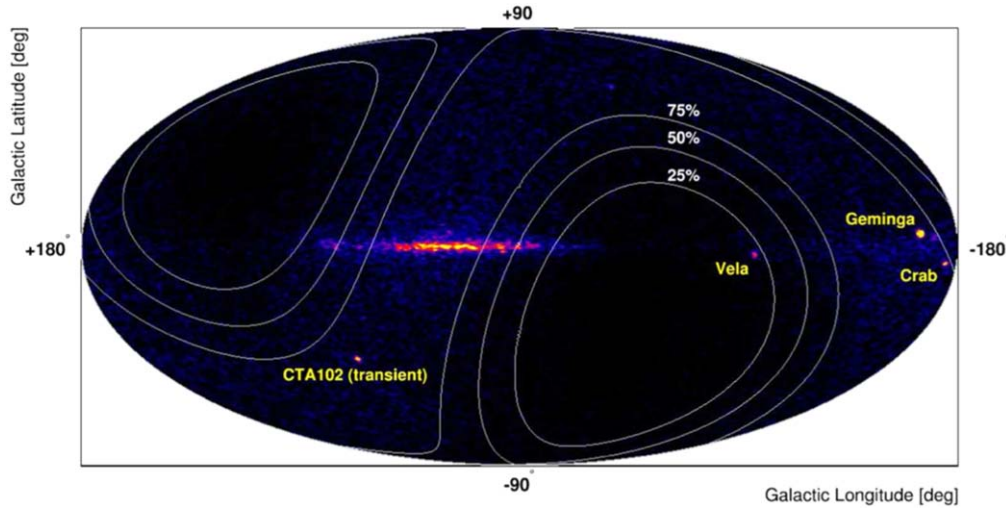


Figure 6. Gamma-ray sky map shown in a Mollweide projection of galactic coordinates [43]. White contours show the relative level of exposure compared to the maximum on the sky. Reproduced from [43]. © IOP Publishing Ltd. All rights reserved.

4.4. Observation of gamma-rays

CALET, with its $30 X_0$ thick calorimeter, has the capability to identify gamma-rays and to measure their energies up to the TeV region. To distinguish gamma rays from charged particles no signals in the CHD and IMC upper layers are required. Moreover, in order to reject upward moving stopping particles, gamma-ray candidates are required to deposit more energy in the bottom layer of the IMC than in the layer of pair conversion. CALET has a dedicated Low-Energy gamma (LE- γ) trigger, that is used to extend the gamma-ray sensitivity down to ~ 1 GeV. In order to avoid an increase of the dead time, this trigger mode is activated only at low geomagnetic latitudes or whenever a gamma-ray burst (GRB) is triggered on-board by the CALET gamma-ray burst monitor (CGBM) [42].

An accurate study of the calorimeter response to gamma-rays has been made comparing simulations and data from the first 24 months of observations [43]. This provides a valuable characterization of the detector performance in terms of effective area, absolute pointing accuracy, angular resolution and Point Spread Function (PSF). The analysis includes also the optimization of event selection criteria, the observation of bright point sources, and the study of diffuse components.

The gamma-ray sky observed by CALET using the LE- γ trigger is shown in figure 6, where galactic emission and bright sources of gamma-rays (the Crab, Geminga, and Vela pulsars and a flare of the AGN CTA 102) are clearly identified. Measured signals from gamma-ray bright point sources and diffuse galactic emission were found to be in agreement with simulated results and expectations from Fermi-LAT data [43], confirming our sensitivity to observe GeV gamma-rays.

Another important observational target for CALET is gamma-ray transients detection, by means of the dedicated CGBM, which can measure the duration and the spectral parameters of GRBs in the energy range from 7 keV up to 20 MeV. As of the end of June 2019, 161 GRBs have been detected by CGBM, with an average rate of ~ 43 GRBs/year, out of which $\sim 12\%$ were classified as short GRBs [44].

Combined analyses of CGBM and calorimeter were performed to search for GeV gamma-rays from confirmed GRBs and for search of electromagnetic counterparts of gravitational waves (GW). At present, for GRBs events based on CGBM, Swift, and Fermi/GBM triggers, no significant counterparts have been detected at >1 GeV [43, 45].

Regarding the counterpart search for gravitational wave events, possible signals compatible with gamma-ray emission were searched, in the calorimeter and CGBM data, on the reported GW151226, GW170104, GW170608, GW170814, and GW170817 events. Upper limits are set on x-ray and gamma-ray counterparts for GW151226 (CAL + CGBM) and GW170104 (CAL), while GW170608, GW170814, GW170817 turned out to be out of the CALET field-of-view [4, 5]. Additional results for counterpart search for the ongoing LIGO/Virgo's Observation Run 3 have been presented in [6].

5. Summary and perspective

CALET was successfully launched on the 19 August 2015, and has been taking data continuously since October 2015, achieving excellent performance and remarkable stability of the instrument. As of 31 May 2019, the total observation time is 1327 days, with a live time fraction close to 84% of

observation time, and more than 860 million events have been collected with HE trigger.

The all-electron spectrum was published in the energy range from 11 GeV to 4.8 TeV [7, 13]. The expected statistics increase by five years of observations (about a factor 3), and a better understanding of systematic uncertainties, will allow us an accurate study of the possible spectral features in the electron spectrum and the flux break above 1 TeV.

The CALET collaboration recently published the direct measurement of the proton spectrum in 50 GeV –10 TeV energy range, the spectral index variation as a function of energy was measured as well, confirming the flux hardening at a few hundred GeV [8]. In the near future, thanks to improved statistics and a better understanding of the instrument, observations might reveal the presence of a charge-dependent energy cutoff in proton and helium spectra, or set important constraints on the acceleration models.

The wide dynamic range of our instrument and its excellent charge identification capability permit the measurement of the energy spectra and composition of CR nuclei up to iron. Preliminary results on primary elements up to ^{26}Fe and secondary-to-primary ratios were already presented in [37–39, 46], and will be published in the near future, addressing important questions in cosmic-ray physics. Such as the universality of the widely observed spectral hardening and the energy dependence of the diffusion coefficient.

Nevertheless, analysis on the relative abundance of UH cosmic-rays up to $Z = 40$ are ongoing [41].

CALET has demonstrated its capability to detect gamma-rays in the energy range from ~ 1 GeV to over 100 GeV, and to observe the diffuse component and bright point-sources in the gamma-ray sky [43].





Moreover, the results obtained in the electromagnetic counterpart search for gravitational wave events [4, 5] demonstrates the great potential of our instrument to perform follow-up observations during the upcoming LIGO/Virgo Observation Run 3.

The so far excellent performance of CALET and the outstanding quality of the data suggest that a 5-year (or more) observation period will most likely provide new interesting results, improving our current knowledge of cosmic-ray phenomena.

Acknowledgments

We gratefully acknowledge JAXA's contributions to the development of CALET and to the operations on-board the ISS. We also wish to express our sincere gratitude to ASI and NASA for their support of the CALET mission.

ORCID iDs

P Brogi  <https://orcid.org/0000-0001-7953-0271>
 K Asano  <https://orcid.org/0000-0001-9064-160X>
 N Cannady  <https://orcid.org/0000-0003-2916-6955>
 H Fuke  <https://orcid.org/0000-0002-8071-3398>

N Mori  <https://orcid.org/0000-0003-2138-3787>

N Ospina  <https://orcid.org/0000-0002-8404-1808>

Y Tsunesada  <https://orcid.org/0000-0001-9238-6817>

References

- [1] Torii S and (for the CALET Collab.) 2017 *PoS (ICRC2017)* **301** 1092
- [2] Torii S and Marrocchesi P S 2019 *Adv. Sp. Res.* **64** 2531–7
- [3] Asaoka Y et al (CALET Collab.) 2019 *J. Phys.: Conf. Ser.* **1181** 012003
- [4] Adriani O et al (CALET Collab.) 2018 *Astrophys. J. Lett.* **863** 160
- [5] Adriani O et al (CALET Collab.) 2016 *Astrophys. J. Lett.* **829** L20
- [6] Mori M et al (CALET Collaboration) 2019 *PoS (ICRC2019)* **358** 586
- [7] Adriani O et al (CALET Collab.) 2018 *Phys. Rev. Lett.* **120** 261102
- [8] Adriani O et al (CALET Collab.) 2019 *Phys. Rev. Lett.* **122** 181102
- [9] Marrocchesi P S et al 2011 *Nucl. Instrum. Methods A* **659** 477
- [10] Marrocchesi P S et al (CALET Collaboration) 2019 *PoS (ICRC2019)* **358** 103
- [11] Brogi P et al 2015 *PoS (ICRC2015)* **236** 595
- [12] Asaoka Y et al (CALET Collab.) 2017 *Astropart. Phys.* **91** 1
- [13] Adriani O et al (CALET Collab.) 2017 *Phys. Rev. Lett.* **119** 181101
- [14] Asaoka Y et al (CALET Collab.) 2018 *Astropart. Phys.* **100** 29
- [15] Asaoka Y et al (CALET Collaboration) 2019 *PoS (ICRC2019)* **358** 001
- [16] Nishimura J et al 1980 *ApJ* **238** 394
- [17] Kobayashi T, Komori Y, Yoshida K and Nishimura J 2004 *Astrophys. J.* **601** 340
- [18] Grimani C 2007 *A&A* **474** 339–43
- [19] Adriani O et al 2009 *Nature* **458** 607
- [20] Accardo L et al (AMS Collaboration) 2014 *Phys. Rev. Lett.* **113** 121101
- [21] Ambrosi G et al (DAMPE Collab.) 2017 *Nature* **552** 63
- [22] Adriani O (PAMELA Collab.) et al 2017 *Riv. Nuovo Cimento* **40** 473–522
- [23] Abdollahi S et al (The Fermi-LAT Collab.) 2017 *Phys. Rev. D* **95** 082007
- [24] Aguilar M et al (AMS Collab.) 2014 *Phys. Rev. Lett.* **113** 221102
- [25] Aharonian F et al (H.E.S.S. Collab.) 2008 *Phys. Rev. Lett.* **101** 261104
- [26] Aharonian F et al (H.E.S.S. Collab.) 2009 *Astron. Astrophys.* **508** 561
- [27] Aguilar M et al (AMS Collab.) 2015 *Phys. Rev. Lett.* **114** 171103
- [28] Aguilar M et al (AMS Collab.) 2015 *Phys. Rev. Lett.* **115** 211101
- [29] Adriani O et al 2011 *Science* **332** 69
- [30] Ahn H S et al 2010 *Astrophys. J. Lett.* **714** L89
- [31] Aguilar M et al (AMS Collab.) 2017 *Phys. Rev. Lett.* **119** 251101
- [32] Haino S et al (BESS Collab.) 2004 *Phys. Lett. B* **594** 35
- [33] Panov A D et al 2007 *Bull. Russ. Acad. Sci. Phys.* **71** 494
- [34] Yoon Y S et al 2011 *Astrophys. J.* **728** 122
- [35] Yoon Y S et al 2017 *Astrophys. J.* **839** 5
- [36] Atkin E et al (NUCLEON Collab.) 2018 *JETP Lett.* **108** 5
- [37] Akaike Y and (for the CALET Collab.) 2019 *J. Phys.: Conf. Ser.* **1181** 012042
- [38] Maestro P 2019 *Adv. Sp. Res.* **64** 2538–45

- [39] Akaike Y *et al* (CALET Collaboration) 2019 *PoS (ICRC2019)* **358** 034
- [40] Murphy R P *et al* 2016 *ApJ* **831** 2083–8
- [41] Rauch B *et al* (CALET Collaboration) 2019 *PoS (ICRC2019)* **358** 130
- [42] Yamaoka K *et al* (CALET Collab.) 2013 *Proc. of the VII Huntsville Gamma-Ray Burst Symposium, GRB 2013, eConf C1304143* 41 (2013)
- [43] Cannady N *et al* (CALET Collab.) 2018 *Astrophys. J. Suppl. S.* **238** 5
- [44] Kawakubo Y *et al* (CALET Collaboration) 2019 *PoS (ICRC2019)* **358** 571
- [45] Cannady N *et al* (CALET Collaboration) 2019 *PoS (ICRC2019)* **358** 557
- [46] Maestro P *et al* (CALET Collaboration) 2019 *PoS (ICRC2019)* **358** 101